Liquid helium cryostat with internal fluorescence detection for x-ray absorption studies in the 2–6 keV energy region

Karen L. McFarlane Holman[a)]
Physical Biosciences Division, Melvin Calvin Laboratory, Lawrence Berkeley National Laboratory, Berkeley, California 94720-5230

Matthew J. Latimer[b)]
Stanford Synchrotron Radiation Laboratory, Stanford University, Stanford, California 94305

Vittal K. Yachandra[c)]
Physical Biosciences Division, Melvin Calvin Laboratory, Lawrence Berkeley National Laboratory, Berkeley, California 94720-5230

(Received 17 June 2003; accepted 16 March 2004; published online 24 May 2004)

X-ray absorption spectroscopy (XAS) in the intermediate x-ray region (2–6 keV) for dilute biological samples has been limited because of detector/flux limitations and inadequate cryogenic instrumentation. We have designed and constructed a new tailpiece/sample chamber for a commercially available liquid helium cooled cryostat which overcomes difficulties related to low fluorescence signals by using thin window materials and incorporating an internal photodiode detector. With the apparatus, XAS data at the Cl, S, and Ca *K* edges have been collected on frozen solutions and biological samples at temperatures down to 60 K. A separate chamber has been incorporated for collecting room-temperature spectra of standard compounds (for energy calibration purposes) which prevents contamination of the cryostat chamber and allows the sample to remain undisturbed, both important concerns for studying dilute and radiation-sensitive samples. © *2004 American Institute of Physics.* [DOI: 10.1063/1.1753672]

I. INTRODUCTION

X-ray absorption spectroscopy (XAS) is an element-specific technique with widespread applications in structural biology, environmental science, and materials chemistry. While obtaining x-ray spectra of solid or concentrated samples is straightforward using transmission mode with ionization chambers, the development of fluorescence detection[1] significantly improved the attainable signal-to-noise thereby facilitating studies of dilute biological and environmental samples. The most widespread use of XAS in biology is to obtain oxidation state and ligand information of metals with x-ray absorption near edge spectroscopy (XANES) and structural information with extended x-ray absorption fine structure (EXAFS) for samples which cannot be or have not yet been crystallized, or to get more precise information about the microstructural environment around the metal center than can be determined using crystallography. These experiments are often performed at the *K* edges of transition metal centers in metalloproteins[2–4] which lie in the ''hard'' x-ray region, $E_{\text{photon}} > 6$ keV.

Sulfur and chlorine are ubiquitous in biological samples, and a more complete development of accessible instrumentation for XAS studies would provide a straightforward technique to probe these atoms that are particularly difficult to study by other spectroscopic methods. Despite subsequent improvements of fluorescence detection methods by the use of energy-resolving detectors,[5] investigations at the *K* edges of low-*Z* atoms such as S and Cl within proteins and other biological samples have remained relatively scarce.[6–10] This is primarily due to the paucity of synchrotron beam lines equipped with wigglers or undulators which provide high flux photons at the *K* edges of these atoms (2–6 keV or ''intermediate'' x-ray energy range), and the lack of beam line instrumentation (cryostat, detector, He flight path, etc.) with which one can perform XAS on dilute (<1 mM) biological samples in this energy region. This article addresses the instrumentation issue, of which the experimenter has direct control. Several papers describing modifications and improvements to XAS cells have been described in the literature,[11–15] but none have presented instrumentation which would facilitate XAS studies at temperatures near liquid helium temperatures to investigate dilute samples of biological interest at the sulfur or chlorine *K* edges (2472 and 2822 eV, respectively). Though existing coldfinger technology is sufficient for samples which can be studied in vacuum, XAS of biological samples is best performed with an ambient pressure of a temperature-exchange gas, usually helium. Biological samples typically have poor thermal conduction and are subject to lyophilization if kept in vacuum. The exchange gas also helps minimize the formation of a ''hot spot'' on the sample, a particularly serious problem for aqueous biological samples at these lower energies where the x-ray beam is almost completely absorbed (>95%) in the first 100 μm of the sample.

Radiation damage is an important consideration for XAS

a)Electronic mail: kholman@willamette.edu; present address: Department of Chemistry, Willamette University, Salem, OR 97301.
b)Electronic mail: latimer@ssrl.slac.stanford.edu
c)Electronic mail: vkyachandra@lbl.gov

TABLE I. Comparison of percent transmission of the incident flux at the sample and fluorescent flux at the detector for iron and sulfur XAS experiments: conventional Oxford Instruments CF1208 cryostat with an external detector vs the new design with an internal photodiode detector or external detector.

Element Chamber/detector configuration	Fe[a] Conventional/ external detector (%)	S[b] Conventional/ external detector (%)	S[b] New design/ external detector (%)	S[b] New design/ photodiode (%)
%T of incident flux to sample at K-edge energy[c]	87	4.0	62	62
%T of fluorescent flux to detector at K_α energy[c,d]	83	2.0	35	100
Total signal reduction due to window materials (as % signal remaining)	72	0.08	22	62

[a]K edge=7112 eV; K_α=6404 eV.
[b]K edge=2472 eV; K_α=2308 eV.
[c]Based on photons passing through two 50-μm-thick Mylar windows for conventional cryostat and two 8-μm-thick Kapton windows for the new design cryostat. Mylar, which is more commonly used with hard x-ray cryostat designs, absorbs comparably to Kapton.
[d]Both fluorescence windows for the new design have an 80% transmittance support grid in addition to an 8-μm-thick Kapton window. The calculations take into account only the effect of window material and support absorptions, not window solid angle, as the impact of that is highly detector dependent.

studies of proteins, cells, tissues, and biological fluids. While some inorganic compounds may be scanned at room temperature with minimal degradation over many hours, one 20 min scan can be enough to degrade a protein, even at 0 °C.[16] Such experiments thus require the use of a liquid helium or liquid nitrogen cryostat with vacuum insulation. In either case helium must be used as the temperature-exchange gas in these experiments because nitrogen would attenuate the incoming and fluorescent x-ray flux considerably. A commonly used commercially available apparatus for hard x-ray XAS is the Oxford Instruments CF1208 liquid helium cryostat equipped with a tailpiece suited for external fluorescence detection with 50–75-μm-thick windows of Al-coated Mylar or Kapton. These windows are excellent in terms of durability, radiation shielding, and vacuum compatibility for hard x-ray experiments but they absorb intermediate-energy x rays significantly. As shown in Table I, at 2470 eV (the sulfur K edge) 4% of the incident photons will arrive at the sample after passing through two 50-μm-thick Mylar windows (a typical thickness for a conventional cryostat used in hard x-ray experiments). However, that is only part of the challenge; detecting the lower energy sample fluorescence signal requires passage through two more windows to reach an external fluorescence detector. The limitations of this experiment are clearly multiplied in the study of dilute samples.

A second problem arises with the typical method used for XAS energy calibration. The monochromatic radiation at a synchrotron beam line is susceptible to energy shifting which necessitates frequent or simultaneous calibration scans during data collection. A common technique is to place a standard sample downstream from the sample and take a simultaneous scan in transmission mode using ionization chamber detection. This method is suitable for hard x rays which easily pass through the sample, but a typical 1-mm-thick sample is essentially opaque for intermediate-energy x rays ($T=1.3\times10^{-13}$% for 1 mm H_2O at 2470 eV, $T=0.029$% at the calcium K edge, 4038 eV). Calibration by running a spectrum of a (concentrated) standard in between sample scans introduces the possibility of contamination of the sample chamber and requires removal and minimally some temperature cycling of the sample.

Several modifications to existing XAS methodology must be made to overcome the aforementioned difficulties of studying dilute samples in the 2–6 keV photon range at liquid helium temperatures: (1) the incident photon flux onto the sample must be maximized by using thin windows which can withstand a 1 atm pressure differential; (2) attenuation of the fluorescence photons must be minimized between the sample and the detector by using thin windows and/or removing unnecessary windows altogether; and (3) provisions should be made for scanning a standard without risk of contamination of the cryostat with the element of interest or disruption or thermal cycling of the sample. Herein we describe an integrated standards sample chamber, liquid helium cryostat tailpiece, and internal detector assembly which was developed to overcome the difficulties inherent to obtaining x-ray absorption spectra of dilute biological samples in this challenging x-ray energy region.

II. EXPERIMENTAL SECTION

A. Sample chamber

The sample chamber has been designed to fit as a tailpiece onto an Oxford Instruments CF1208 liquid helium cryostat, but with simple modifications it could be used with other types of cryostats. Details of the inner sample chamber and its outer shroud are shown in Fig. 1. All components are machined from aluminum except where noted. The x-ray entrance window on the outer shroud is 8-μm-thick Kapton (polyimide), which is mounted with epoxy onto a detachable window plate which seals to the outer shroud with a polybutyl rubber o ring. The entrance window into the sample chamber is 8-μm-thick Kapton coated with 0.2 μm diamondlike carbon (DLC) by Crystallume, Santa Clara, CA. We

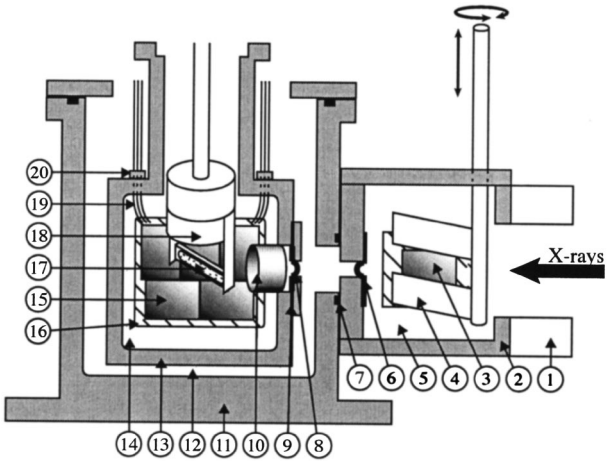

FIG. 1. Side view of the sample and standard chambers. (1) entrance port downstream from the I_o ion chamber and slits; (2) Al standard chamber; (3) Si photodiode; (4) retractable flaps for mounting standards; (5) He atmosphere; (6) 8-μm-thick polyimide window; (7) butyl rubber o ring; (8) 8 μm polyimide window with 0.2 μm diamond-like carbon coating; (9) indium o-ring seal; (10) Al pipe scatter snout; (11) Al outer sample chamber; (12) vacuum space; (13) Al inner sample chamber; (14) 1 atm He gas; (15) five Si photodiode array; (16) photodiode array mount; (17) sample; (18) sample rod; (19) polyimide-coated wires for photodiode signal output; and (20) indium-sealed electrical throughput (detailed in Fig. 2).

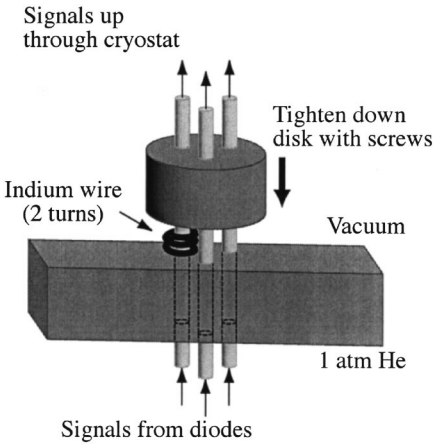

FIG. 2. Electrical throughput. Wires are sent through holes (snug fit) in the chamber wall and an Al disk. Two turns of 1 mm diameter indium wire are wrapped around each wire and the disk is tightened down to the chamber.

have found that using Kapton windows with a DLC coating reduced difficulties with He diffusion. The internal sample chamber window was mounted with epoxy onto a plate which is mounted onto the chamber with an indium seal. Both entrance windows accommodate the beam spot (approx. 12 mm width×1 mm height) on beam line VI-2 at the Stanford Synchrotron Radiation Laboratory.

A short pipe (''scatter snout'') is affixed to the inside of the sample chamber window. This piece shields the internal photodiode detectors from scattered radiation caused by the incoming beam striking the entrance window, thus lowering the background current signal.

The outer and inner chambers are rectangular shaped, in contrast to conventional XAS cryostat designs where a cylindrical sample compartment allows for closer proximity of the sample to an external detector. Our design is more suitable for an internal detector array of several photodiodes mounted flat against one of the inner walls at 90° to the incident window. The opposite wall is a detachable solid plate with an indium seal which can be interchanged with a plate containing a large window with a thin (8 μm) film and a support grid for use with an external detector. The support grid was necessary because the fluorescence windows are too large (3.5 in. diameter for the outer chamber) for the thin film to withstand a 1 atm pressure differential. Although a grid of different composition could be used, we used an Al grid machined in-house which transmits 80% of the flux. The fluorescence window option is for detector flexibility; to use an external detector exclusively and at hard x-ray energies, the conventional cylindrical design should be used.

B. Photodiode detector assembly

The silicon photodiode array was fabricated by International Radiation Detectors, Inc., Torrance, CA. It consists of five AXUV-300 diodes mounted onto a Kovar plate with a mixture of standard and conductive epoxies to insure grounding. Each diode has its own cathode to enable discrimination of each signal separately. All electrical connections were made using indium solder. The diode array is mounted onto the inside wall of the sample chamber with an aluminum mounting plate which has male connector pins, one for each diode and several redundant pins for the common anode (ground). The mounting plate with connector pins allows for simple assembly and removal of the detector from the sample chamber for cleaning purposes.

Because dilute samples generate signal currents in the picoampere range, the wire length between the photodiodes and the amplifiers is minimized and the wires are shielded as much as possible. The Kapton-coated stainless steel wires are fed through the wall of the inner sample chamber as shown in Fig. 2. Although copper wire could be used, stainless steel was chosen since its thermal conductivity is ~28 times less than that of copper and we wanted to minimize heat transfer into the cryostat's inner chamber. A small helix (2–3 turns) of indium wire is wrapped around the wire, and a small aluminum disk with holes for passage of the wires is tightened down against the outer chamber wall to create a vacuum-tight electrical feedthrough suitable down to 10 K. The signal wires follow the length of the cryostat and exit out the top to minimize thermal loss from the sample chamber.

C. Standards chamber

A separate chamber for running XAS spectra of standard compounds for energy calibration was designed to fit onto the front of the sample chamber and is kept purged with He gas. The standard compound were spread onto Mylar tape with a <10-μm-thick polypropylene cover, and taped onto a retractable flap within the chamber. For scanning a standard, the flap is lowered into the beam path. A silicon photodiode (AXUV-300M, IRD, Inc.) is used as the detector. This method enables one to easily scan a standard in between several scans of the same sample without disruption or addi-

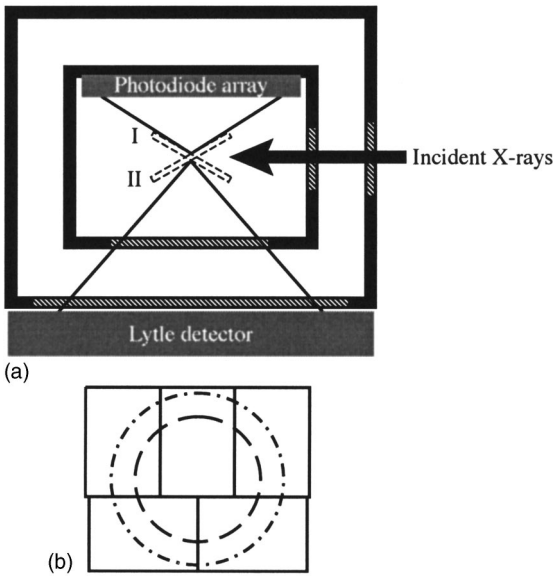

FIG. 3. Comparison of fluorescence signals for internal and external detectors. When the sample is in either position I or II shown in Fig. 3(a), fluorescence x rays originate from the illuminated sample in the direction of the internal photodiode detector (position I) or passes through two windows to reach an external detector (position II). This figure demonstrates that a larger solid angle is achieved within a shorter distance for the photodiode configuration. The relationship is shown more quantitatively in Fig. 3(b) where the photodiode array face is shown with the cross sections at the same distance of the windows for the standard and modified design superimposed. The dash-dot line is the standard cryostat window (90° cone from sample center) and the dashed line is the new design (72° cone from sample center). The photodiode array clearly accepts the largest solid angle of fluorescence.

tional x-ray exposure of the cooled sample, or risk of contamination of the sample chamber.

III. RESULTS AND DISCUSSION

Figure 3 presents a comparison of the solid angle for the internal detector and an external fluorescence detector[17] using the standard or new rectangular design. The currently available cylindrical design allows for closer proximity of an external detector with good solid angle but it lacks space for a windowless internal detector. The internal detector has a larger accessible solid angle of fluorescence photons, comparable to that obtainable with a cylindrical design [see Fig. 3(b)]. The solid angle afforded by the thin supported windows is the smallest of the three, but is only envisioned to be used with an energy-resolving detector which is more limited usually by its own acceptance. The size of the supported external windows in the new design are adequate for a standard Canberra 13-element Ge detector. In addition, if the detector geometry is known and the position fixed relative to the cryostat, supports can be designed which will give only the attenuation of the window materials, further enhancing efficiency of the fluorescence detection. Such an optimization was not attempted in the present study.

The superiority of the internal detector in terms of flux can be seen by comparing the percent transmittance of the incidence x rays as they pass through the windows of the sample chamber, interact with the sample, and then fluoresce and reach the detector. Table I displays comparative values for percent transmittance of the initial flux at two locations in

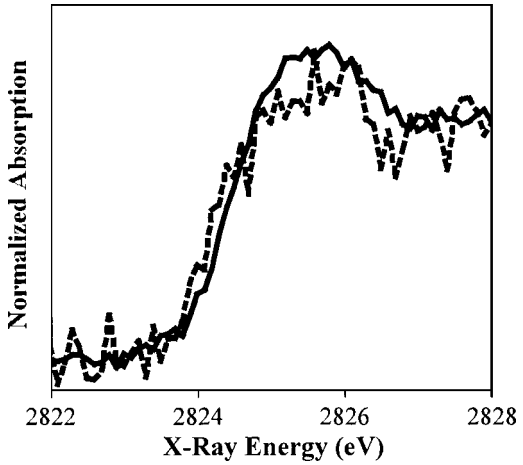

FIG. 4. Normalized chlorine *K*-edge x-ray absorption spectra of a 250 μM chloride solution in 50% glycerol, one scan (dashed line); and an inactive Photosystem II membrane-bound protein complex in a 50% glycerol/buffer solution, 30-scan average (solid line). Spectra were collected at 60 K using the internal photodiode array assembly.

the sample chamber, at the sample and at the detector, for the conventional hard x-ray design and the new design. These values were calculated with a program by E. Gullikson at the Center for X-Ray Optics, Lawrence Berkeley National Laboratory, available at the web site http://www-cxro.lbl.gov. The calculations are based upon a mix of experimental measurements and theoretical calculations and determine the transmittance based on the absorption and scattering cross sections of individual atomic constituents of the material.

The conventional cryostat is acceptable for experiments at higher energies (e.g., the iron *K* edge), but clearly would not suffice for sulfur XAS regardless of the absorber concentration. The new design with an external detector is much better, but for dilute samples there still may be difficulties since the two fluorescence windows severely attenuate the signal. The internal photodiode detection system is comparable to the standard hard x-ray experiment, with no attenuation of the fluorescence photon flux, just the attenuation of the photons passing through the entrance windows.

Other factors being equal, the internal photodiodes are comparable to a Lytle detector used with the standard cryostat (comparable active area with no energy discrimination). External energy resolving detectors are commonly used for dilute samples in the hard x-ray region, where incident beam and fluorescence photons can more readily pass through window materials. For dilute samples in the intermediate energy range, an energy-resolving detector might also be favored in terms of signal to noise but the loss of fluorescence signal to cryostat window absorption can make such measurements impractical. In such cases, an internal photodiode may be the only way in which one may detect the element of interest for XAS experiments.

To test the system, we obtained Cl *K*-edge spectra at 60 K of dilute aqueous solutions of chloride at various concentrations down to 250 μM and inactivated Photosystem II (PS II) membranes where [Cl]=~250 μM. Figure 4 presents the Cl *K*-edge spectrum of a single scan of a 250 μM chloride solution in 50% (v/v) glycerol and a signal-averaged spec-

trum (30 scans) of inactive PS II samples in 50% (v/v) glycerol. The signal-to-noise ratio for a single scan is undesirable for analysis or presentation purposes but is included to show that a Cl *K*-edge spectrum of this relatively low chloride concentration is observable within one scan using this apparatus. Such concentrations are challenging even for experiments in the hard x-ray range and to our knowledge, XAS detection of such dilute samples is unprecedented in the intermediate x-ray region.

We have also used the apparatus at the sulfur *K* edge for distinguishing between disulfides and thiol groups in sulfur-containing protein samples at 90 K.[18] Calcium EXAFS was investigated[19] for the oxygen-evolving complex of PS II at 100 K using the fluorescence window with support grid and an energy-resolving Ge detector.

It is important to collect XAS data on biological samples at low temperatures in order to protect them from radiation damage. In testing the temperature range of the apparatus, 10 K was the lowest temperature that was reached. None of the 10 K data is presented here due to difficulties with a lower signal-to-noise ratio for those samples and problems with stability/reproducibility. Incorporating a radiation shield into the design would allow for a more stable apparatus at lower temperatures and would also reduce He consumption.

ACKNOWLEDGMENTS

This work was supported by grants from the Director, Office of Basic Energy Sciences, Division of Energy Biosciences of the U.S. Department of Energy (DOE), under Contract No. DE-AC03-76SF00098, and by the National Institutes of Health (GM55302). Synchrotron radiation facilities were provided by the Stanford Synchrotron Radiation Laboratory (SSRL) which is operated by the Department of Energy, Office of Basic Energy Sciences. The SSRL Biotechnology Program is supported by the National Institutes of Health, National Center of Research Resources, Biomedical Technology Program, and by the Department of Energy, Office of Health and Environmental Research. The authors would like to express their gratitude to Dr. Roehl Cinco, Dr. John Robblee, Dr. Hendrik Visser, Dr. Carmen Fernandez, Dr. Emanuele Bellacchio, Dr. Shelly Pizarro, and Dr. Johannes Messinger for their tireless efforts and creativity during the development of the cryostat. They also thank Professor Ken Sauer for his helpful suggestions, Dr. Hendrik Visser and Jerry LaRue for their assistance with the drawings, and Mike Press for his electrical prowess. Last but most importantly, this publication would not have been possible without the guidance, foresight and ingenuity of our dear colleague and friend Melvin P. Klein, 1921–2000.

[1] J. Jaklevic, J. A. Kirby, M. P. Klein, A. S. Robertson, G. S. Brown, and P. Eisenberger, Solid State Commun. **23**, 679 (1977).
[2] V. K. Yachandra, Methods Enzymol. **246**, 638 (1995).
[3] S. P. Cramer, in *Biochemical Application of X-Ray Absorption Spectroscopy*, edited by D. C. R. P. Koningsberger (Wiley, New York, 1988), pp. 257–320.
[4] R. A. Scott, in *X-Ray Absorption Spectroscopy*, edited by D. L. Rousseau (Academic, Orlando, FL, 1984), pp. 295–362.
[5] S. P. Cramer, O. Tench, M. Yocum, and G. N. George, Nucl. Instrum. Methods Phys. Res. A **266**, 586 (1988).
[6] S. E. Shadle, J. E. Penner-Hahn, H. J. Schugar, B. Hedman, K. O. Hodgson, and E. I. Solomon, J. Am. Chem. Soc. **115**, 767 (1993).
[7] A. Rompel *et al.*, Proc. Natl. Acad. Sci. U.S.A. **95**, 6122 (1998).
[8] I. J. Pickering, R. C. Prince, T. Divers, and G. N. George, FEBS Lett. **441**, 11 (1998).
[9] A. Bianconi, A. Giovannelli, L. Gastellani, S. Alema, P. Fasella, B. Oesch, and S. Mobilio, J. Mol. Biol. **165**, 125 (1983).
[10] C. Holt, S. S. Hasnain, and D. W. L. Hukins, Biochim. Biophys. Acta **719**, 299 (1982).
[11] L. R. Furenlid, M. W. Renner, and J. Fajer, Rev. Sci. Instrum. **61**, 1326 (1990).
[12] F. W. H. Kampers, T. M. J. Maas, J. van Grondelle, P. Brinkgreve, and D. C. Konigsberger, Rev. Sci. Instrum. **60**, 2635 (1989).
[13] E. Sanchez Marcos, M. Gil, J. M. Martinez, A. Munoz-Paez, and A. Sanchez Marcos, Rev. Sci. Instrum. **65**, 2153 (1994).
[14] F. Villain, V. Briois, I. Castro, C. Helary, and M. Verdaguer, Anal. Chem. **65**, 2545 (1993).
[15] S. Weber, A. E. Ostafin, and J. R. Norris, Rev. Sci. Instrum. **69**, 2127 (1998).
[16] B. Chance, W. Pennie, M. Carman, V. Legallais, and L. Powers, Anal. Biochem. **124**, 248 (1982).
[17] F. W. Lytle, R. B. Greegor, D. R. Sandstrom, E. C. Marques, J. Wong, C. L. Spiro, G. P. Huffman, and F. E. Huggins, Nucl. Instrum. Methods Phys. Res. A **226**, 542 (1984).
[18] E. Bellacchio, K. L. McFarlane, A. Rompel, J. H. Robblee, R. M. Cinco, and V. K. Yachandra, J. Synchrotron Radiat. **8**, 1056 (2001).
[19] R. M. Cinco, K. L. McFarlane Holman, J. H. Robblee, J. Yano, S. A. Pizarro, E. Bellacchio, K. Sauer, and V. K. Yachandra, Biochemistry **41**, 12928 (2002).